


Greatly enhanced flux pinning properties of fluorine-free metal–organic decomposition YBCO films by co-addition of halogens (Cl, Br) and metals (Zr, Sn, Hf)

Takanori Motoki^{1,5} , Shuhei Ikeda¹, Shin-ichi Nakamura², Genki Honda³, Tatsuoki Nagaishi³, Toshiya Doi^{4,5} and Jun-ichi Shimoyama^{1,5}

¹ Department of Physics and Mathematics, Aoyama Gakuin University, 5-10-1 Fuchinobe, Chuo-ku, Sagami-hara, Kanagawa 252-5258, Japan

² TEP Co. Ltd, 2-20-4 Kosuge, Katsushika-ku, Tokyo 124-0001, Japan

³ Sumitomo Electric Industries Ltd, 1-1-3 Shimaya, Konohana-ku, Osaka 554-0024, Japan

⁴ Graduate School of Energy Science, Kyoto University, Yoshida-honmachi, Sakyo-ku, Kyoto 606-8501, Japan

⁵ JST-ALCA, Chiyoda-ku, Tokyo 102-0076, Japan

E-mail: motoki@phys.aoyama.ac.jp

Received 12 January 2018, revised 8 February 2018

Accepted for publication 12 February 2018

Published 6 March 2018



Abstract

Additive-free YBCO films, as well as those with halogen (X) added, metal (M) added and (X , M) co-added, have been prepared by the fluorine-free metal–organic decomposition method on $\text{SrTiO}_3(100)$ single crystalline substrates, where $X = \text{Cl, Br}$ and $M = \text{Zr, Sn, Hf}$. It was revealed that the addition of both Cl and Br to the starting solution resulted in the generation of oxyhalide, $\text{Ba}_2\text{Cu}_3\text{O}_4\text{X}_2$, in the YBCO films, and that the oxyhalide was found to promote the bi-axial orientation of the YBCO crystals. By adding a decent amount of Cl or Br, highly textured YBCO films with high J_c were reproducibly obtained, even when an impurity metal, M , was co-added, while the addition of M without X did not greatly improve J_c owing to the poor bi-axial orientation of the YBCO crystals. Our results suggest that the addition of Br more effectively enhances J_c than the addition of Cl. The pinning force density at 40 K in 4.8 T reached $\sim 55 \text{ GN m}^{-3}$ with the co-addition of (Br, M). This value is much larger than that of the pure YBCO film, reaching $\sim 17 \text{ GN m}^{-3}$.

Keywords: YBCO, fluorine free MOD, BMO-addition, thin films, oxyhalide, Ba2342, flux pinning

(Some figures may appear in colour only in the online journal)

Introduction

The preparation methods of $\text{REBa}_2\text{Cu}_3\text{O}_y$ (REBCO, RE: rare earth element) thin films and coated conductors have been vigorously developed, and the major processes can be classified into four approaches: pulsed laser deposition (PLD), metal–organic chemical vapor deposition (MOCVD), reactive co-evaporation by deposition and reaction (RCE-DR) and metal–organic decomposition (MOD). In recent years, REBCO tapes 100 m long with high critical current properties have been

commercially produced by adopting these methods. In order to expand the application fields, it is highly necessary to reduce the cost of the manufacturing process and improve the critical current density (J_c) in the magnetic fields of the tapes.

One of the most cost-effective methods of manufacturing REBCO tapes is a solution-based method, MOD, in which neither vacuum chambers nor high-power laser devices are needed. The MOD method, which uses trifluoroacetates as the starting materials, known as TFA-MOD, has been extensively studied, since highly textured films showing a high J_c can be

reproducibly obtained through reactions of the precursor including BaF_2 or Ba-O-F amorphous phases. It is reported that a pseudo-liquid phase appears at the interface of the growth front during crystallization, and therefore bi-axially oriented REBCO films are formed even when second phases or impurities co-exist [1]. However, this generally requires a relatively long heat treatment time of more than a few hours under precisely controlled water vapor pressure [2]. In addition, impurity oxides tend to cover the film surface, which makes it difficult to prepare a stabilizing Ag layer cap with homogeneous electrical and physical contacts. This is partially because the TFA-MOD solution usually starts with a Ba-deficient stoichiometry in the preparation of high-quality REBCO films [3, 4].

MOD-processed REBCO films starting with fluorine-free solutions, called the fluorine-free MOD (FF-MOD) method, have also been developed by many groups, since REBCO crystals form in a very short time without the generation of any harmful gases such as HF [5–12]. Our group has reported that sintering of only 1 min is enough for the preparation of textured YBCO films [5]. Since homogeneous films with flat and clean surfaces are obtained by using the FF-MOD method, thick films can be prepared by re-coating the solution and then carrying out pyrolysis on the previously sintered films. Honda *et al* successfully prepared YBCO films 4.7 μm thick on buffered metal substrates without any cracks [6]. Regarding these points, FF-MOD is one of the most promising methods for manufacturing REBCO tapes. However, the inhomogeneous decomposition of BaCO_3 in the precursor film during the crystallization process brings about a narrow range of optimal sintering conditions and relatively low reproducibility. The J_c of the FF-MOD-processed REBCO films is high enough $>10^6 \text{ A cm}^{-2}$ at 77 K in low fields. However, this decreases rapidly with an increase in external magnetic fields compared with REBCO films prepared by other methods, such as PLD and TFA-MOD, probably owing to the lack of effective pinning centers introduced during film growth. Furthermore, the addition of impurity nanoparticles or nanorods, such as BaMO_3 ($M = \text{Zr, Sn, Hf, etc.}$), which is known to be one of the most effective ways of improving the flux pinning properties of REBCO films prepared by the PLD [13, 14], MOCVD [15] and TFA-MOD [16, 17] methods, cannot be easily applied to FF-MOD-processed REBCO films, because the addition of impurity metals usually disturbs the formation of the bi-axially oriented REBCO matrix. Nonetheless, among the numerous attempts on FF-MOD-processed REBCO films, several groups have succeeded in enhancing the flux pinning properties by adding BaMO_3 nanoparticles such as BaZrO_3 [7], BaHfO_3 [8–10] and BaSnO_3 [10].

Our previous studies revealed that the addition of Cl to the starting solution resulted in the generation of bi-axially oriented oxychloride, $\text{Ba}_2\text{Cu}_3\text{O}_4\text{Cl}_2$, without decreasing T_c [9, 10]. It is notable that oxychloride promotes the crystallization of YBCO, unlike other impurities, and improves the J_c reflecting the high crystallinity without randomly oriented grains in the film. Moreover, the addition of Cl was found to be extremely effective in extending the sintering conditions to lower temperatures and shorter sintering times [11]. These results are promising for the development of long and

homogeneous REBCO tapes by suppressing reactions between the REBCO and buffered oxide layers.

In this study, we have conducted further investigations on the addition of halogen elements and impurity metals to enhance the flux pinning properties. Kipka *et al* reported that Br as well as Cl can be introduced to the halogen sites X of $\text{Ba}_2\text{Cu}_3\text{O}_4\text{X}_2$ sintered bulks [18]. The successful synthesis of the $\text{Ba}_2\text{Cu}_3\text{O}_4(\text{Cl}_{0.5}\text{Br}_{0.5})_2$ -sintered bulk in the same report suggests that $\text{Ba}_2\text{Cu}_3\text{O}_4\text{X}_2$ with $X = \text{Cl}$ and Br is the perfect miscible system. Hereafter, $\text{Ba}_2\text{Cu}_3\text{O}_4\text{X}_2$ will be abbreviated as Ba2342 considering the compositional ratio of this oxyhalide. It should be noted that Ba2342 compounds with halogen elements except Cl and Br, i.e. F or I, have not been reported thus far.

Firstly, we focus on the effect that adding Br to YBCO films has on their crystallinity and superconducting properties compared to those of additive-free YBCO films and those with Cl added. Then, the effects of adding X (Cl, Br) and/or M (Zr, Sn, Hf) on the flux pinning properties are investigated. Most of the previous studies on the effects of adding BaMO_3 on FF-MOD-processed REBCO films focus on the mono metal element, such as $M = \text{Zr}$. Therefore, the difference in the effects of the impurity metal elements has not been well clarified in the FF-MOD method. In the present study, all combinations of (X, M), where $X = \text{Cl, Br}$ and $M = \text{Zr, Sn, Hf}$, are inclusively studied with varying the doping level of M .

Experimental

Propionate-based solutions with nominal compositions of $\text{YBa}_{2+2x}\text{Cu}_{3+3x}\text{O}_y\text{X}_{2x}\text{M}_z$ ($X = \text{Cl, Br, } M = \text{Zr, Sn, Hf, } x = 0, 0.05, z = 0\text{--}0.05$) were prepared. Cl, Br and M were added by mixing hydrochloric acid, hydrobromic acid and M -solution supplied by High Purity Chemicals Co. Ltd, respectively. The total cation concentration of the solution was controlled at 1 mol l^{-1} . Green films were formed by spin-coating (3000 rpm for 10 s) the solution on the $\text{SrTiO}_3(100)$ single crystalline substrates in air and calcining them at $\sim 500^\circ\text{C}$ under flowing oxygen with $P_{\text{H}_2\text{O}} \sim 2.1 \text{ kPa}$ moisture to remove organic components. These coating and calcination processes were repeated three times to increase the film thickness. Then, the films were heated in a tube furnace up to 780°C with a ramping rate of $10^\circ\text{C min}^{-1}$ and held for 1 h under an O_2/Ar mixed gas flow with a P_{O_2} of 10 Pa. Finally, the films were annealed at 450°C for 12 h under oxygen flow and quickly cooled to room temperature to control the oxygen composition of the YBCO in the optimally doped state of the carrier. Detailed synthesis conditions can be found elsewhere [9]. Additive-free YBCO films, as well as those with X added, M added and (X, M) co-added, were inclusively prepared with a final film thickness of $\sim 400 \text{ nm}$.

The constituent phases of the films and the crystallinity of the YBCO were investigated by the surface x-ray diffraction (XRD) method with θ - 2θ scanning using a RIGAKU Ultima IV. The surface and cross-sectional microstructures of the films were observed by a scanning electron microscope (SEM, KEYENCE VE-7800) and a 400 kV transmission electron microscope (TEM, JEOL JEM-4010), respectively.

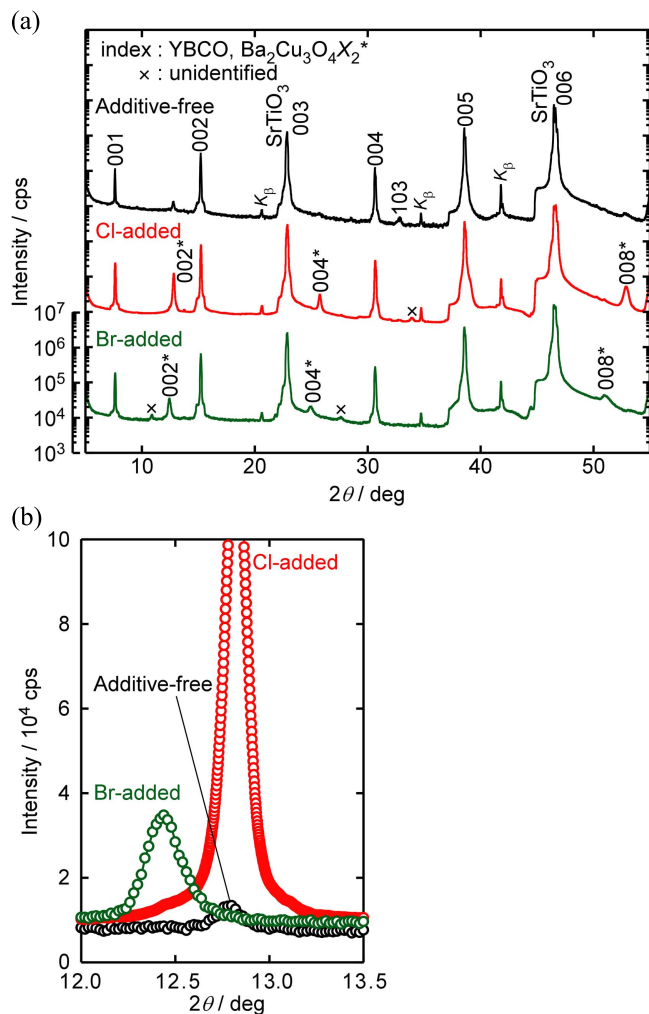


Figure 1. The surface XRD patterns of additive-free YBCO films as well as those with Cl and Br added (a); an enlarged view around the 002($\text{Ba}_2\text{Cu}_3\text{O}_4\text{X}_2$) peak (b). Peak shifts in the 00l($\text{Ba}_2\text{Cu}_3\text{O}_4\text{X}_2$) diffractions are observed following the addition of Br compared to the film with Cl added, which demonstrates that Br is introduced to the halogen sites X of $\text{Ba}_2\text{Cu}_3\text{O}_4\text{X}_2$.

Magnetic susceptibility and magnetization hysteresis loops were measured at 77 K and 40 K using a SQUID magnetometer (Quantum Design MPMS XL-5s) under dc fields up to 5 T. In these measurements, magnetic fields were always applied normal to the film surface, i.e. parallel to the *c*-axis of the epitaxially grown YBCO films. J_c values were calculated using the extended Bean model assuming a film thickness of 400 nm for all the samples.

Results and discussion

The surface XRD patterns of the additive free YBCO films as well as those with Cl and Br added, prepared by the FF-MOD method, are shown in figure 1(a). Strong 00l peaks of YBCO are observed for all films including the one with Br added, which indicates that YBCO films with a strongly aligned *c*-axis were successfully prepared in sintering conditions of

780 °C, $P_{\text{O}_2} = 10$ Pa, 1 h. It should be noted that the 103 (YBCO) peak, which reflects the existence of randomly oriented YBCO grains in the film, appears only in the additive-free one. This means that the generation of randomly oriented grains is suppressed by the addition of Cl or Br, which is consistent with our previous results where the crystallinity of YBCO is enhanced by the addition of Cl [9, 10]. In addition, sharp peaks of 00l($\text{Ba}_2\text{342}$) were observed in the XRD patterns of the YBCO films with Cl or Br added. Figure 1(b) shows an enlarged view around the 002 ($\text{Ba}_2\text{342}$) peak of each sample, which indicates that the 2θ of the 002($\text{Ba}_2\text{342}$) peak is located at a lower angle for the film with Br added. This demonstrates that Br has been successfully introduced to the halogen sites X of the $\text{Ba}_2\text{Cu}_3\text{O}_4\text{X}_2$ compounds. It should be noted that the 2θ position of the 002 peak of pure $\text{Ba}_2\text{Cu}_3\text{O}_4\text{Br}_2$ is approximately 12.1° considering the study of the sintered bulks [18]. However, the 2θ position of the 002($\text{Ba}_2\text{342}$) peak of the Br-added YBCO film appears in the middle of the peak positions between pure $\text{Ba}_2\text{Cu}_3\text{O}_4\text{Cl}_2$ and $\text{Ba}_2\text{Cu}_3\text{O}_4\text{Br}_2$, which originates from the existence of a trace amount of Cl in the starting materials to enhance the stability of the solution. In other words, oxybromides, $\text{Ba}_2\text{Cu}_3\text{O}_4(\text{Cl},\text{Br})_2$, with Cl partially substituted were generated in the film with Br added. The estimated composition calculated from the 2θ value is $\text{Ba}_2\text{Cu}_3\text{O}_4(\text{Br}_{0.54}\text{Cl}_{0.46})_2$ for this film. The existence of weak peaks due to $\text{Ba}_2\text{342}$ in the pattern of the additive-free YBCO film originates for the same reason.

Figures 2(a) and (b) show the surface and cross-sectional microstructures of the YBCO film with Br added, respectively. The surface of the film is flat and some rectangular-shaped precipitates can be observed. These precipitates, with a size of a few to tens of micrometers were confirmed to be $\text{Ba}_2\text{342}$ by elemental analysis. Note that low levels of Cl as well as Br were detected in the $\text{Ba}_2\text{342}$ precipitates, which provides supporting evidence for the systematic peak shift of 00l($\text{Ba}_2\text{342}$) shown in figure 1. The edge directions of all the rectangular $\text{Ba}_2\text{342}$ crystals shown in figure 2(a) are almost identical, i.e. each edge of the $\text{Ba}_2\text{342}$ precipitates is rotated $\sim 45^\circ$ from the crystallographic axes of SrTiO_3 corresponding to the *a*(*b*)-axis of the epitaxially grown YBCO. This can be explained by the lattice matching between $\text{SrTiO}_3/\text{Ba}_2\text{342}$ and YBCO/ $\text{Ba}_2\text{342}$. $\text{Ba}_2\text{342}$ has a layered tetragonal crystal structure, $I4/mmm$, in which cuprate Cu_3O_4 -planes exist like CuO_2 planes in the YBCO. Therefore, good lattice matching is achieved when $\text{Ba}_2\text{342}$ is rotated 45° against the YBCO in the *ab*-plane. The matching pseudo-lattice constant of $\text{Ba}_2\text{342}$ —in this case the distance of the nearest Cu-Cu atoms in the Cu_3O_4 planes—becomes ~ 3.9 Å, although the lattice constant of the *a*-axis of $\text{Ba}_2\text{342}$ is in the range 5.52–5.54 Å depending on the (Cl, Br) ratio in the halogen sites. It should be noted that the *a*-axis length of $\text{Ba}_2\text{342}$ is almost unchanged by the (Cl, Br) ratio, while that of the *c*-axis varies greatly from 13.82–14.56 Å according to the (Cl, Br) ratio. From the discussion above, it is considered that $\text{Ba}_2\text{342}$ crystals are bi-axially oriented in the YBCO film, and this was actually

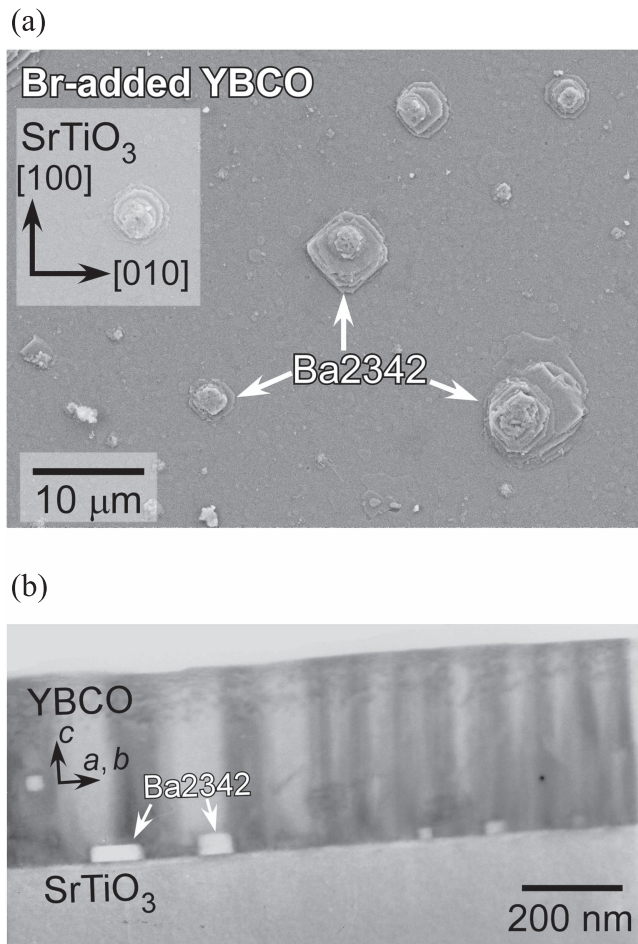


Figure 2. A surface SEM image (a) and a cross-sectional TEM image (b) of the YBCO film with Br added. Rectangular parallelepiped precipitates, Ba2342, are observed in both the surface and the cross-section of the film.

confirmed by the observation of four-fold symmetry peaks using in-plane XRD measurements.

The cross-sectional microstructure shown in figure 2(b) indicates that a homogeneous YBCO film with a flat surface was obtained when Br was added to the starting solution. Rectangular-shaped precipitates, as shown by arrows in figure 2(b), which were mainly observed at the interface of YBCO/SrTiO₃, were considered to be Ba2342 precipitates. The size of Ba2342 largely differs from that observed on the surface of the film in figure 2(a), which suggests the widely distributed size of the Ba2342 precipitates from tens of nanometers to tens of micrometers. Also, the contrasting vertical stripes, corresponding to twin boundaries, were observed to be continuous from the substrate to the surface of the film, which indicates that the YBCO was biaxially oriented. These observations on the surface and cross-section of the YBCO film with Br added are consistent with our previous studies about the addition of Cl to YBCO films [9, 10].

The temperature dependence of magnetization and the magnetic field dependence of the J_c of additive-free YBCO films, as well as those with Cl and Br added, are shown in figures 3(a) and (b), respectively. In figure 3(a), sharp

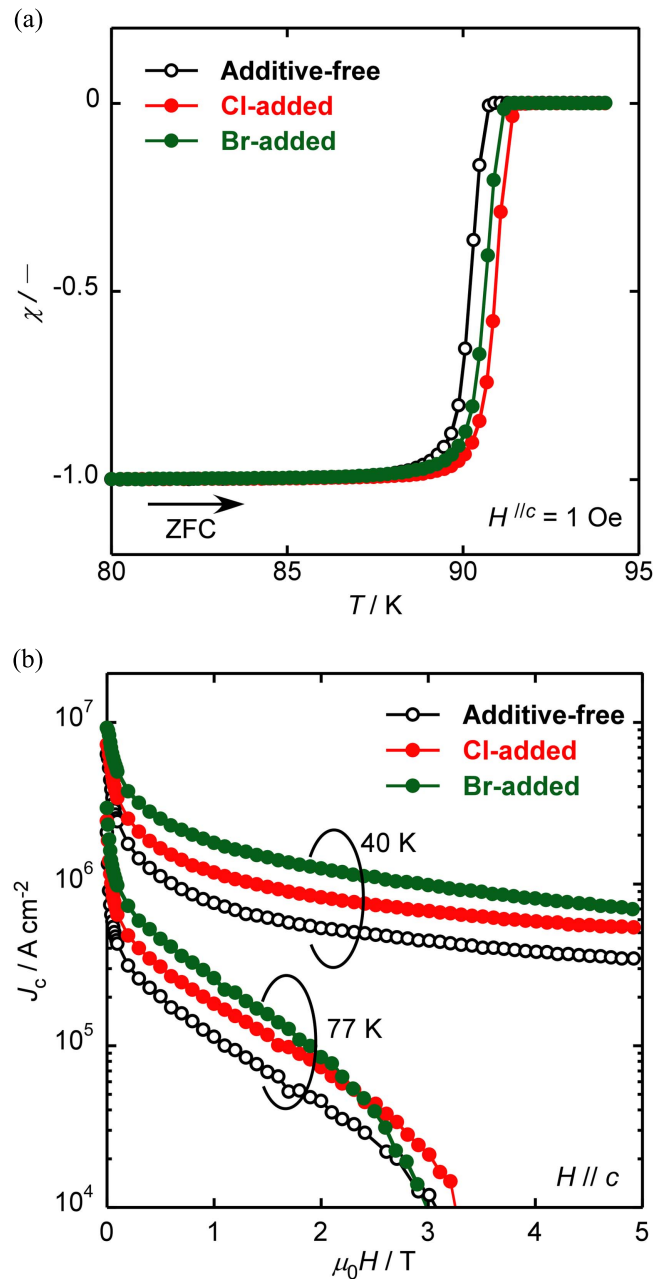


Figure 3. The temperature dependences of magnetization (a) and the magnetic field ($H//c$) dependences of J_c (b) of additive-free YBCO films as well as those with Cl and Br added.

superconducting transitions with a T_c of ~ 91.5 K were observed for the YBCO films with Cl or Br added, which means that the oxygen sites of the YBCO were not substituted by the halogen elements. On the other hand, the additive-free YBCO film showed a slightly lower T_c of ~ 90.8 K, probably owing to the strains induced by misoriented grains in the film, which is indicated by the appearance of a 103(YBCO) peak shown in figure 1(a). J_c - H curves shown in figure 3(b) mean that adding both Cl and Br improve the J_c in all applied fields, especially at 40 K. It was revealed that the addition of Br was more effective at enhancing the flux pinning properties than the addition of Cl. Although the intrinsic reasons for this difference have not been clarified yet, YBCO films with Br

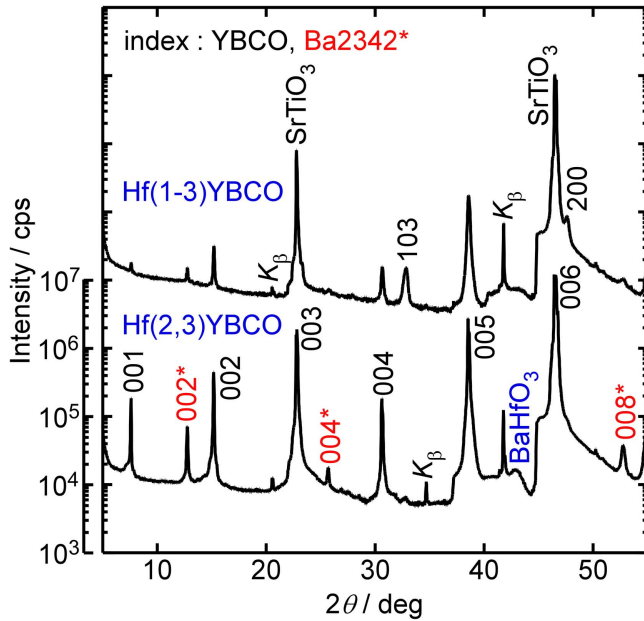


Figure 4. The surface XRD patterns of (Cl, Hf) co-added YBCO films prepared in two different calcination conditions.

added have better crystallinity than those with Cl added, not to mention the additive-free ones. This idea that the addition of Br promotes the bi-axial alignment of YBCO better is consistent with the results of the co-addition of metals described in the latter part of this paper.

The addition of impurity metals, such as Zr, Sn and Hf, combined with halogen elements was conducted in order to further enhance the flux pinning properties by the introduction of fine BaMO_3 particles in the film. As a preliminary study, the co-addition of Cl and Hf with the nominal composition of $\text{Y}:\text{Ba}:\text{Cu}:\text{Cl}:\text{Hf} = 1:2 + 2x:3 + 3x:2x:z$ ($x = 0.05$, $z = 0.01$) was attempted in two ways as follows. One way involved the preparation of the film by coating a (Cl, Hf) co-added solution on all three layers, while the other involved coating a Hf-free solution with Cl added to the first layer—i.e. the layer on top of the substrate—and the (Cl, Hf) co-added solution to the second and third layers. Hereafter, these two films will be expressed as Hf(1-3)YBCO and Hf(2,3)YBCO, respectively. Figure 4 shows the surface XRD patterns of these two (Cl, Hf) co-added films. For the Hf(1-3)YBCO film, the 00l(YBCO) peaks were relatively weak and a large 103(YBCO) peak was observed. On the other hand, YBCO with a strong c -axis alignment was obtained for the Hf(2,3)YBCO film with a very weak 103(YBCO) peak. It is suggested that metal impurities—in this case Hf—added to the first layer of the calcination film suppressed the epitaxial growth of both YBCO and $\text{Ba}_2\text{342}$, and therefore the epitaxial growth of YBCO proceeded imperfectly. On the basis of this preliminary study, hereafter the addition of M was conducted for the second and third layers of the calcination film, just like the preparation methodology of the Hf(2,3)YBCO film. It should be noted that the average doping level of M in a whole film is two thirds of the doping level of each layer with M added.

By applying this methodology described above, YBCO films with the addition of all combinations of (X , M), where $X = \text{Cl}$, Br and $M = \text{Zr}$, Sn, Hf, were systematically prepared

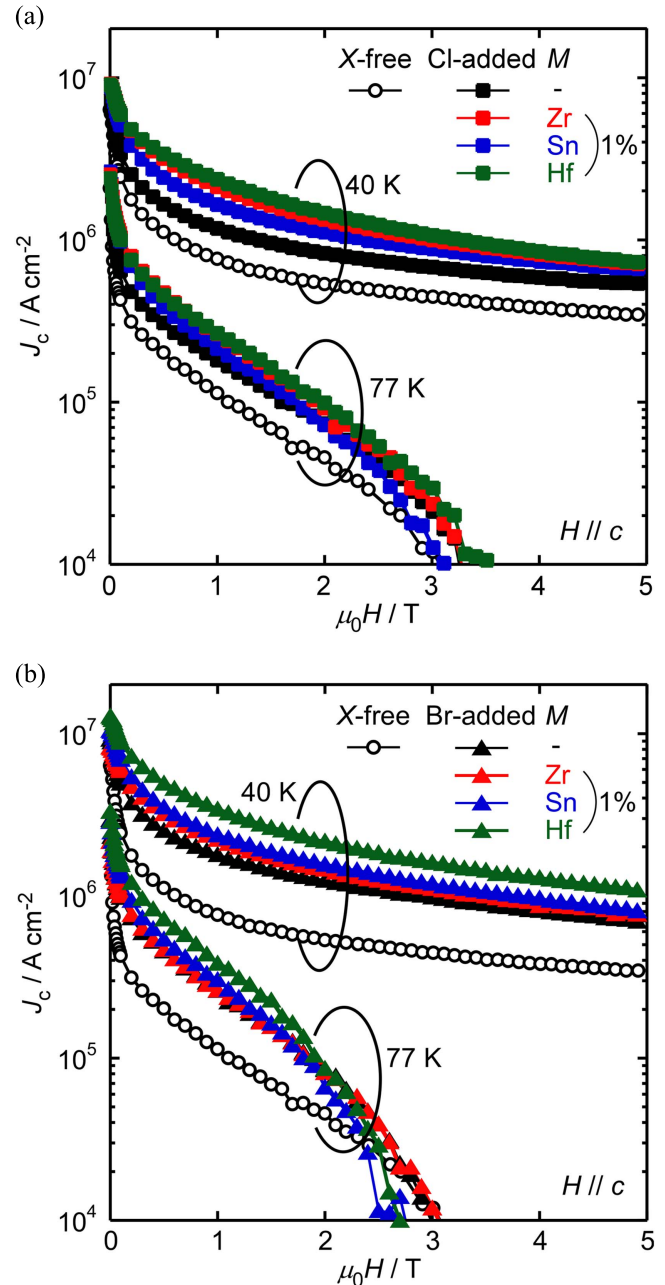


Figure 5. The magnetic field ($H//c$) dependences of J_c of (Cl, 1 mol% M) co-added (a) and (Br, 1 mol% M) co-added (b) YBCO films.

with the doping level of M fixed at 1 mol%. Figures 5(a) and (b) show the J_c dependences of the magnetic field at 77 K and 40 K of (Cl, 1 mol% M) co-added (a) and (Br, 1 mol% M) co-added (b) YBCO films compared with a pure YBCO film, respectively. By comparing the pure film with (X , M) co-added films, any combination of (X , M) is effective to markedly improve the J_c properties. In particular, the co-addition of Br and M is found to be more effective than the co-addition of (Cl, M).

In order to quantitatively estimate the flux pinning properties systematically, YBCO films with different doping levels of M (0.5–5 mol%) and 1 mol% films with M added, without the addition of halogen elements, were also prepared

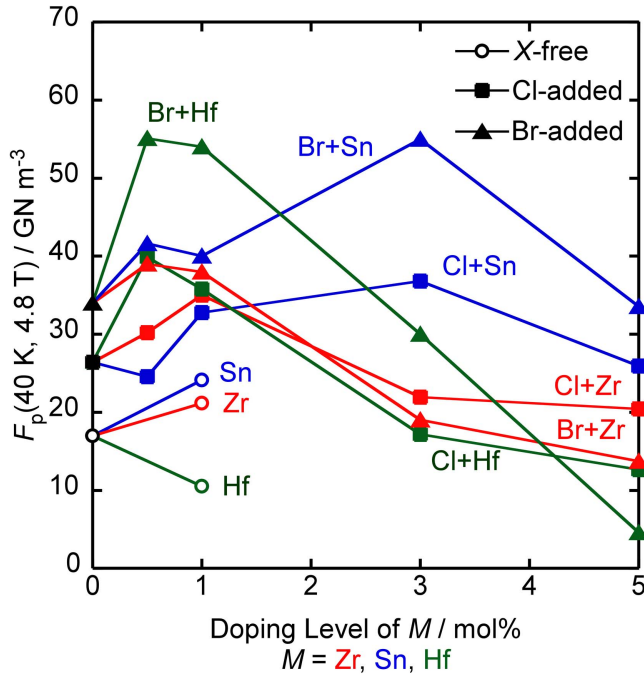


Figure 6. The summarized pinning force densities, F_p (40 K, 4.8 T), of the additive-free YBCO films, as well as those with X added, M added and (X, M) co-added with different doping levels of M of 0–5 mol%, where $X = \text{Cl, Br}$ and $M = \text{Zr, Sn, Hf}$.

under the same conditions, where the addition of M was only conducted for the second and third layers of the calcination films as mentioned before. It can be said that the c -axis-oriented YBCO films were successfully prepared for all combinations, and they showed a high $T_c > 90$ K, although the T_c gradually drops with an increase in the doping level of M , e.g. YBCO films with Cl+Hf1%, Cl+Hf3%, Cl+Hf5% co-added showed a $T_{c,\text{onset}}$ of 91.2 K, 91.0 K and 90.3 K, respectively. In the case of adding BaMO_3 to the REBCO films by the PLD method, Tsuruta *et al* reported that T_c monotonically drops with an increase in the BaMO_3 content regardless of the variation in M of Zr, Hf and Sn, which is due to the expansion of the YBCO lattice by the tensile stresses induced in the lattice-mismatched interfaces [19]. The observed gradual decrease in T_c in the present study is considered to be due to the increasing strains induced both by misoriented YBCO grains and BaMO_3 nanoparticles. Figure 6 summarizes the F_p (40 K, ~ 4.8 T) of the additive free, X -added, M -added and (X, M) co-added YBCO films. Here, it was shown that the addition of M without X did not greatly improve F_p , up to $\sim 24 \text{ GN m}^{-3}$, compared with the value of a pure YBCO film $\sim 17 \text{ GN m}^{-3}$. On the other hand, the co-addition of X and M was found to be very effective at enhancing the flux pinning properties up to $\sim 55 \text{ GN m}^{-3}$ for the (Br, 0.5% Hf) or (Br, 3% Sn) co-added films, which is more than triple that of the additive-free film. Considering our previous reports [9, 10], dispersed fine BaMO_3 particles were considered to be introduced by the co-addition of (X, M) and act as strong pinning centers. Figure 7 shows the relationship

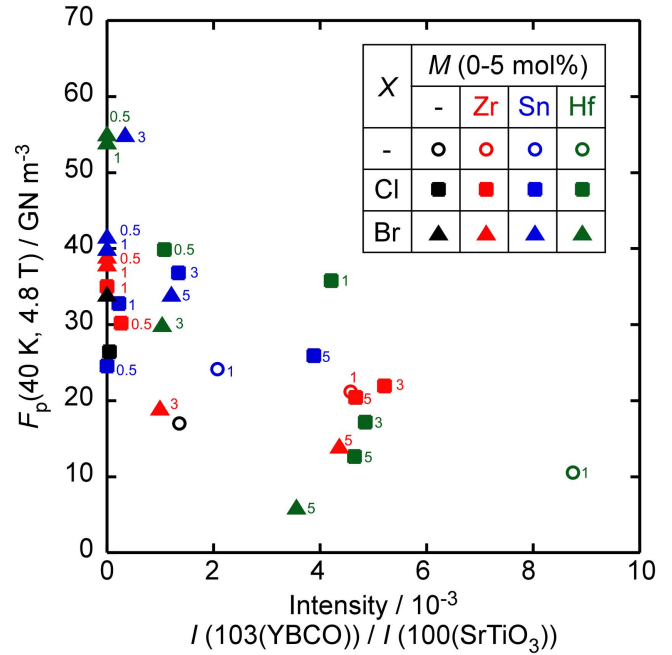


Figure 7. The relationship between F_p (40 K, 4.8 T) and the normalized intensities of the 103(YBCO) peaks of additive-free YBCO films, as well as those with X added, M added and (X, M) co-added, with different doping levels of M , where $X = \text{Cl, Br}$ and $M = \text{Zr, Sn, Hf}$. The number beside each plot indicates the doping level of M .

between F_p (40 K, 4.8 T) as summarized in figure 6, as well as the intensities of the 103(YBCO) peak, which reflect the degree of misorientation. Each 103(YBCO) peak intensity is evaluated by surface XRD θ - 2θ scanning and normalized by each 100(SrTiO_3) peak intensity considering slight differences in the size of the measured films. Through analysis, the addition of X is confirmed to be effective for suppressing the generation of randomly oriented grains compared with X -free films, even when impurity metals are co-added. Also, there is a tendency for the appearance of the 103(YBCO) peak to greatly deteriorate the flux pinning properties. The intensity of the 103(YBCO) peak systematically increases with an increase of the doping level of M , which can account for the degradation of F_p at a high doping level of M . It was found that the optimal doping level of M differs from the element of M that forms BaMO_3 . The tendency is in this order: $\text{Hf} < \text{Zr} < \text{Sn}$, i.e. the addition of Sn disturbs the bi-axial orientation of the YBCO matrix the least, and therefore a relatively high concentration ~ 3 mol% is effective. This trend almost corresponds to the degree of lattice mismatch between YBCO and BaMO_3 , e.g. +8.3% for $\text{BaHfO}_3/\text{YBCO}$ and +6.9% for $\text{BaSnO}_3/\text{YBCO}$. In the case of co-adding (X, M) , it can be said that the addition of Br more effectively enhances the flux pinning properties than adding Cl, although Cl as well as Br almost perfectly suppress the disorder of the YBCO matrix when the doping level of M is low enough.

Finally, the effects of adding Br will be discussed compared to adding Cl. We prepared pure $\text{Ba}_2\text{Cu}_3\text{O}_4\text{X}_2$ ($X = \text{Cl}, \text{Br}$) films from the organic-solvent-based solution with nominal compositions of $\text{Ba}:\text{Cu}:X = 2:3:2$ in order to investigate the growth mechanism of Ba2342. It was found that Ba2342 films with the c -axis aligned for both $X = \text{Cl}$ and Br can be successfully obtained on SrTiO_3 single crystalline substrates at sintering temperatures as low as 550°C for 1 h in $P_{\text{O}_2} = 10$ Pa. These results demonstrate that Ba2342 crystals with both $X = \text{Cl}$ and Br are epitaxially grown in the early stage of the sintering process of YBCO films with X added, and therefore, they promote the bi-axial alignment of the YBCO matrix. Regarding these points, there may be a few differences in the growth condition of Ba2342 depending on the halogen elements. However, a major difference was revealed when YBCO films with (Br, M) co-added were prepared with a (Br, M) coating co-added solution for all three calcination layers, just like the previously described Hf(1-3) YBCO film. In contrast to the (Cl, Hf) co-added (Hf(1-3) YBCO) film shown in figure 4, films with a strongly aligned c -axis were reproducibly obtained with doping levels of M up to 1 mol%. These results will be addressed in detail in future publications. Based on the results and discussion above, although the intrinsic mechanism has not been clarified yet, the addition of Br evidently promotes the bi-axial orientation of YBCO better than the addition of Cl.

Conclusions

Additive-free YBCO films, as well as those with halogen (X) added, metal (M) added and (X, M) co-added ($X = \text{Cl}, \text{Br}$ and $M = \text{Zr}, \text{Sn}, \text{Hf}$) were prepared by a fluorine-free MOD method. By adding X , oxyhalide, $\text{Ba}_2\text{Cu}_3\text{O}_4\text{X}_2$, with a c -axis orientation was generated in the film, which is considered to promote the bi-axial alignment of YBCO and improve J_c properties, reflecting the good crystallinity. Moreover, great improvements were achieved by co-adding both X and M . The addition of Br was found to be more effective at enhancing the flux pinning properties than the addition of Cl, especially when the dilute impurity metal M was co-added. The pinning force density at 40 K in 4.8 T reached up to $\sim 55 \text{ GN m}^{-3}$ by co-addition of (Br, M) compared with that of the pure film $\sim 17 \text{ GN m}^{-3}$. The addition of Br is promising for the further development of FF-MOD-processed REBCO films as it compatibly achieves the enhancement of both the crystallinity and flux pinning properties.

Acknowledgments

Part of this work was supported by the ALCA project of the Japan Science and Technology Agency (JST) and by the JSPS KAKENHI, grant numbers 16H07161 and 17K14814.

ORCID iDs

Takanori Motoki  <https://orcid.org/0000-0003-3218-0977>

References

- [1] Araki T and Hirabayashi I 2003 *Supercond. Sci. Technol.* **16** R71–94
- [2] Teranishi R, Tanaka T, Matsuda J, Nakaoka K, Izumi T, Shiohara Y, Mori N and Mukaida M 2010 *Mater. Sci. Eng. B* **173** 61–5
- [3] Shiohara Y, Fujiwara N, Hayashi H, Nagaya S, Izumi T and Yoshizumi M 2009 *Physica C* **469** 863–7
- [4] Zhang H L, Ding F Z, Gu H W, Dong Z B, Qu F and Shang H J 2016 *J. Supercond. Nov. Magn.* **29** 1227–32
- [5] Ishiwata Y, Shimoyama J, Motoki T, Kishio K and Nagaishi T 2013 *IEEE Trans. Appl. Supercond.* **23** 7500804
- [6] Honda G et al 2011 *Abstr. CSJ Conf.* **84** 187 (in Japanese)
- [7] Lu F, Kametani F and Hellstrom E E 2013 *Supercond. Sci. Technol.* **26** 045016
- [8] Kobayashi N, Kita R and Miura O 2017 *IEEE Trans. Appl. Supercond.* **27** 8001104
- [9] Motoki T, Shimoyama J, Yamamoto A, Ogino H, Kishio K, Honda G and Nagaishi T 2014 *Supercond. Sci. Technol.* **27** 095017
- [10] Motoki T et al 2016 *Supercond. Sci. Technol.* **29** 015006
- [11] Motoki T, Ikeda S, Honda G, Nagaishi T, Nakamura S and Shimoyama J 2017 *Appl. Phys. Express* **10** 023102
- [12] Zhao Y, Chu J, Qureshi T, Wu W, Zhang Z, Mikheenko P, Johansen T H and Grivel J C 2018 *Acta Mater.* **144** 844–52
- [13] Horide T, Taguchi K, Matsumoto K, Matsukida K, Ishimaru M, Mele P and Kita R 2016 *Appl. Phys. Lett.* **108** 082601
- [14] Yoshida Y, Miura S, Tsuchiya Y, Ichino Y, Awaji S, Matsumoto K and Ichinose A 2017 *Supercond. Sci. Technol.* **30** 104002
- [15] Xu A, Delgado L, Khatri N, Liu Y, Selvamanickam V, Abrahimov D, Jaroszynski J, Kametani F and Larbalestier D C 2014 *APL Mater.* **2** 046111
- [16] Palau A, Bartolomé E, Llordés A, Puig T and Obradors X 2011 *Supercond. Sci. Technol.* **24** 125010
- [17] Miura M, Maiorov B, Willis J O, Kato T, Sato M, Izumi T, Shiohara Y and Civale L 2013 *Supercond. Sci. Technol.* **26** 035008
- [18] Kipka R and Müller-Buschbaum H 1976 *Z. Anorg. Allg. Chem.* **424** 1–4
- [19] Tsuruta A, Yoshida Y, Ichino Y, Ichinose A, Matsumoto K and Awaji S 2014 *J. Phys. Conf. Ser.* **507** 022043